Co- and Posttranslational Modification of the α_{1B}-Adrenergic Receptor: Effects on Receptor Expression and Function†

Katja Björklöf,‡ Kenneth Lundström,§ Liliane Abuin,‡ Peter J. Greasley,‡ and Susanna Cotecchia*,‡

Institut de Pharmacologie et Toxicologie, Université de Lausanne, 1005 Lausanne, Switzerland, and F. Hoffmann-La Roche Reasearch Laboratories, 4070 Basel, Switzerland

Received September 21, 2001; Revised Manuscript Received January 15, 2002

ABSTRACT: We have characterized the maturation, co- and posttranslational modifications, and functional properties of the α_{1B}-adrenergic receptor (AR) expressed in different mammalian cells transfected using conventional approaches or the Semliki Forest virus system. We found that the α_{1B}-AR undergoes N-linked glycosylation as demonstrated by its sensitivity to endoglycosidases and by the effect of tunicamycin on receptor maturation. Pulse−chase labeling experiments in BHK-21 cells demonstrate that the α_{1B}-AR is synthesized as a 70 kDa core glycosylated precursor that is converted to the 90 kDa mature form of the receptor with a half-time of approximately 2 h. N-Linked glycosylation of the α_{1B}-AR occurs at four asparagines on the N-terminus of the receptor. Mutations of the N-linked glycosylation sites did not have a significant effect on receptor function or expression. Surprisingly, receptor mutants lacking N-linked glycosylation migrated as heterogeneous bands in SDS−PAGE. Our findings demonstrate that N-linked glycosylation and phosphorylation, but not palmitoylation or O-linked glycosylation, contribute to the structural heterogeneity of the α_{1B}-AR as it is observed in SDS−PAGE. The modifications found are similar in the different mammalian expression systems explored. Our findings indicate that the Semliki Forest virus system can provide large amounts of functional and fully glycosylated α_{1B}-AR protein suitable for biochemical and structural studies. The results of this study contribute to elucidate the basic steps involved in the processing of G protein-coupled receptors as well as to optimize strategies for their overexpression.

The α_{1B}-adrenergic receptor (AR)[1] belongs to the large superfamily of G protein-coupled receptors (GPCRs) that transduce a variety of signals across the cell membrane. GPCRs are structurally characterized by seven transmembrane α-helices connected by alternating extracellular and intracellular loops. The N-terminus is extracellular, and the C-terminus lies within the cytosol. The extracelluar half is involved in ligand binding and contributes to the stabilization of the structure of the receptors. Sequences on the cytosolic surface mediate the interaction of the receptor with G proteins as well as regulatory and signaling proteins like protein kinases and arrestins. Rhodopsin was recently crystallized, and it is the only GPCR whose crystal structure has been so far solved (*1*).

Co- and posttranslational modifications can influence the structure, function, and expression of GPCRs. These include, for example, glycosylation, phosphorylation, and palmitoylation.

The role of N-glycosylation has been studied in a number of GPCRs. Removal of this modification by site-directed mutagenesis or by biochemical approaches resulted in different effects on various receptors. For some receptors, including the hamster β_2-AR (*2*), the receptor for platelet activating factor (*3*), the rat lutropin receptor (*4*), the human thyrotropin receptor (*5*), the human calcium receptor (*6*), the human dopamine D5 (*7*), and the rat EP3 receptor for prostaglandin E2 (*8*) and for the human AT_{1a} for angiotensin II receptor (*9*), it has been shown that N-linked glycosylation is important for the expression at the plasma membrane. In contrast, mutations of the N-linked glycosylation sites did not have any effect on the expression of the canine H2 histamine receptor (*10*), the receptor for human parathyroid hormone (*11*), and the human V2 vasopressin receptor (*12*). Generally, N-linked glycosylation did not seem to play an important role in receptor function for most GPCRs. However, mutations of the N-glycosylation sites impaired the coupling of rhodopsin to transducin (*13*). In a recent study on fly rhodopsin it was shown that N-linked glycosylation was important for the interaction of the receptor with its chaperone NinaA, even though the mature receptor did not contain any N-linked glycosylation (*14*). Recently, it was also shown that the V2 vasopressin receptor, the δ opioid

† This work was supported by the Fonds National Suisse de la Recherche Scientifique (Grant 31-51043.97) and by the European Community (Grant BMH4-CT98-3566).

* To whom correspondence should be addressed at the Institut de Pharmacologie et de Toxicologie, Faculté de Médecine, 27 Rue du Bugnon, 1005 Lausanne, Switzerland. Tel: 41-21-692 5400. Fax: 41-21-692 5355. E-mail: susanna.cotecchia@ipharm.unil.ch.

‡Université de Lausanne.

§ F. Hoffmann-La Roche Reasearch Laboratories.

[1] Abbreviations: AR, adrenergic receptor(s); GPCR, G protein-coupled receptor; SFV, Semliki Forest virus; PAGE, polyacrylamide gel electrophoresis; BHK-21, baby hamster kidney 21; HEK-293, human embryonic kidney 293; DMEM, Dulbecco's modified Eagle's medium; [^{125}I]HEAT, [^{125}I]iodo-2-[β-(4-hydroxyphenyl)ethylaminomethyl]tetralone; PNGase F, peptide:*N*-glycosidase F; Endo H, endoglycosidase H; AP, alkaline phosphatase.

10.1021/bi015790j CCC: $22.00
Published on Web 03/05/2002

receptor, and octopus rhodopsin can undergo O-linked glycosylation next to N-linked glycosylation (*15*−*17*). However, for the vasopressin and opioid receptors neither one of these modifications had an impact on the functional properties of the receptors.

The effects of receptor phosphorylation have been the focus of a number of studies (for review, see ref *18*). Phosphorylation of several GPCRs most commonly results in the uncoupling of the receptors from G proteins, thus representing an important step in receptor desensitization.

Receptor palmitoylation has been shown for a few GPCRs, including the human β_2-AR (*19*), the human α_{2A}-AR (*20*), the human A1 adenosine receptor (*21*), and the rat bradikinin B2 receptor (*22*). The palmitate group is linked in these receptors to conserved cysteines in the proximal portion of the C-terminus, which is postulated to be inserted in the lipid bilayer. The recent crystal structure of bovine rhodopsin (*1*) supports this hypothesis. The positioning of helix 8 in the crystal structure fits with a potential insertion of the two palmitate groups into the lipid bilayer and may thus define an important functional domain of the receptor. Depalmitoylation of the β_2-AR was shown to be a prerequisite of receptor phosphorylation and desensitization (*23*).

Most GPCRs are expressed at low levels in tissues and need efficient overexpression systems in order to obtain enough protein suitable for biochemical and structural studies. However, using mammalian overexpression systems membrane proteins often reveal structural heterogeneity resulting from various co- and posttranslational modifications and incomplete processing. This heterogeneity can depend on the cells as well as on the transfection system that is used for the overexpression of the receptor. Because of the growing need to obtain large amounts of GPCRs for structural studies, it has become important to characterize the processing of various receptors expressed in different recombinant systems.

In this study we have characterized the co- and posttranslational modifications of the α_{1B}-AR as well as their functional implications in different mammalian cells transfected using conventional approaches or the Semliki Forest virus (SFV) system. The first aim of this work is to characterize the basic steps involved in receptor maturation that have not been extensively investigated so far for the α_{1B}-AR. The second goal is to optimize the conditions for receptor overexpression.

EXPERIMENTAL PROCEDURES

Materials. Alkaline phosphatase, complete protease inhibitor cocktail, and Pwo DNA polymerase were from Roche Diagnostics (Basel, Switzerland). DMEM, Ham's F-12 and Iscove's medium, gentamicin, fetal calf serum, endoglycosidase H (Endo H), peptide:*N*-glycosidase F (PNGase F), and restriction enzymes were from Life Technologies, Inc. (Grand Island, NY). [^{3}H]Glucosamine, [^{3}H]galactose, [^{125}I]HEAT, [^{3}H]inositol, and [^{125}I]iodoarylazidoprazosin were from DuPont-New England Nuclear (Boston, MA). [^{35}S]Methionine, anti-rabbit HRP antibody, and ECL Western blotting detection reagent were from Amersham Pharmacia Biotech; adrenaline was from Sigma (St. Louis, MO). Protein assay (Bradford) was from Bio-Rad Laboratories GmbH (Germany). Effectene was from Qiagen AG (Switzerland). The TNT quick-coupled transcription/translation system was from Promega Corp. (Madison, Wl).

DNA Constructs and Site-Directed Mutagenesis. The cDNA encoding the hamster α_{1B}-AR was tagged with a six-histidine epitope at the C-terminus by subcloning it in-frame into the vector pET21a. The resulting construct was subcloned into pSFV-1 expression vector used to generate the virus. Mutagenesis was performed by PCR using mismatch primers and Pwo polymerase on the cDNA subcloned in the pRK5 expression vector used for transfections. Mutations were confirmed by automated DNA sequencing (Microsynth, Switzerland). To construct the receptor−GFP fusion proteins, the cDNA encoding the α_{1B}-AR or its mutants was subcloned into the pE-GFP-N1 using *Eco*RI/*Age*I. The cDNA of fusion proteins were subsequently subcloned into pRK5 using *Eco*RI/*Xba*I.

Cell Culture. BHK-21 cells were grown in a mixture of Ham's F-12 and Iscove's (1:1) medium supplemented with 10% fetal calf serum and gentamycin (100 μg/mL). Rat-1 fibroblasts, HEK-293, and COS-7 cells were grown in high-glucose DMEM supplemented with 10% fetal calf serum and gentamicin (100 μg/mL). For viral infection and transient transfection cells were split the day before the infection/transfection into six-well dishes (300000−500000 cells/well) or in 100 mm dishes [(1−2) $\times$ 10^6 cells/dish].

Semliki Forest Virus (SFV) Stock Preparation and Viral Infection. In vitro transcripts and in vivo packaging of recombinant SFV particles were carried out as previously described (*24*). BHK-21 cells confluent at 60−70% were infected with 0.1 mL of virus ($\sim 10^8$ infective units/mL) in 0.5 mL of medium per six-well dish. After 2 h, the medium containing the virus was removed, and fresh medium was added (*25*). At 16 h postinfection experiments were performed as described below.

Effectene Transfections. Effectene transfections were carried out according to the manufacture's protocol with 40−50% confluent cells. Optimized conditions for all cell lines used in this study were 0.8 μg of DNA and 8 μL of effectene per well of six-well dishes (300000−500000 cells) and 4 μg of DNA and 40 μL of effectene per 100 mm dish [(1−2) $\times$ 10^6 cells]. Cells were harvested 24 h after the transfection. In the case of the tunicamycin treatment, tunicamycin was added immediately after the transfection to a final concentration of 5 μg/mL.

Membrane Preparations. Transfected or infected cells were lysed in 5 mM Tris-HCl, pH 7.4, at 4 °C, and 5 mM EDTA supplemented with complete protease inhibitor cocktail, and total cellular membranes were centrifuged at 40000*g* for 20 min. After treatment with 10 μg/mL DNase I in the presence of 10 mM $MgCl_2$, membranes were frozen in liquid N_2 and stored at −80 °C. Protein concentration was determined using the Bio-Rad protein assay. Membrane preparations were used for ligand binding, Western blotting, and photoaffinity labeling.

Ligand Binding. Ligand binding assays on membrane preparations using [^{125}I]HEAT were performed as described (*26*). Prazosin (10^{-6} M) was used to determine nonspecific binding. [^{125}I]HEAT concentration was 250 pM for measuring receptor expression at a single concentration and 80 pM for competition binding analysis. For saturation binding experiments the concentration of the radioligand was 12−400 pM. Saturation analysis and competition curves were

analyzed using Prism 3.02 (GraphPad, Software Inc., San Diego, CA).

Inositol Phosphate Measurement. Transfected or infected cells were labeled for 12 h with myo[^{3}H]inositol at 4 μCi/mL in inositol-free DMEM supplemented with 1% fetal bovine serum. Cells were then preincubated for 10 min in PBS containing 20 mM LiCl and then stimulated for 45 min with adrenaline. Total inositol phosphates were extracted and separated as described previously (*26*).

Metabolic Labeling of Cells. Cells grown in six-well dishes (300000−500000 cells/well) were washed twice with PBS and preincubated with 1.5 mL of methionine-free DMEM medium for 30 min. Cells were then labeled for 20 min with 0.4 mL of the same medium containing 100 μCi/mL [^{35}S]-methionine (1000 Ci/mmol). After the pulse, cells were subjected to different chase periods as indicated using methionine-free medium supplemented with 1 mM cold methionine up to 1 h of chase and complete medium for longer chase periods. For labeling with [^{3}H]glucosamine or [^{3}H]galactose cells were preincubated with 2 mL of DMEM medium containing 1000 mg/L glucose and labeled for 5−6 h using 0.4 mL of the same medium containing 70 μCi/mL radiolabeled sugar. Labeled cells were lysed in buffer A (50 mM Tris-HCl, pH 7.4, at 4 °C, 150 mM NaCl, 2 mM EDTA, 1% NP-40) supplemented with complete protease inhibitor cocktail for 30 min on ice. The cell lysate was collected and frozen in liquid N_2 and stored at −80 °C. After being thawed, the cell lysate was centrifuged at 15000*g* for 15 min, and the supernatant was kept for immunoprecipitation.

Immunoprecipitation of the Receptors. For quantification of the radioactivity, the supernatants from cells metabolically labeled were precipitated with 10% (w/v) TCA, and the radioactivity in the precipitate was counted. For each labeled sample, an aliquot containing 500000 dpm was immunoprecipitated. The immunoprecipitation was carried out overnight in buffer A including 2.5% (w/v) protein A−Sepharose and receptor-specific rabbit polyclonal antibodies (1:250). The antibody used in all of the experiments shown was raised against a glutathione *S*-transferase fusion protein encoding the C-terminal portion of the α_{1B}-AR beyond residue S356. This antibody was a kind gift of Prof. Hitoshi Kurose (University of Tokyo). In some experiments, we also used a polyclonal antibody raised against the first 22 amino acids of the N-terminus of the α_{1B}-AR as previously described (*27*).

Endoglycosidase and Alkaline Phosphatase Treatments. Endoglycosidase treatment was carried out on membrane preparations or on solubilized membranes using PNGase F (final concentration 5 units/μL) and Endo H (final concentration 10 units/μL) in the buffers recommended by the manufacturer at room temperature for 12−14 h. For immunoprecipitation of the receptor after endoglycosidase treatment, the samples were diluted 10-fold with buffer A, and immunoprecipitation was carried out as described above. For alkaline phosphatase treatment, the samples were first denatured using 0.25% SDS and 0.5% β-mercaptoethanol. Calf intestine alkaline phosphatase was added to a final concentration of 0.05 unit/μL, and the mixture was incubated for 1.5 h at 37 °C in the buffer provided.

SDS−PAGE and Western Blotting. SDS−PAGE was performed using 8−13% gradient gels. Membranes were denatured in the SDS−PAGE sample buffer (65 mM Tris, pH 6.8, 2% SDS, 5% glycerol, 5% β-mercaptoethanol) for 60 min at room temperature. For Western blotting, the SDS−PAGE was followed by electroblotting onto nitrocellulose membranes. The blots were incubated for 1 h at room temperature with the same antibody against the C-terminus of the receptor used for immunoprecipitation diluted 1:1000. After the antiserum was washed, the membranes were incubated with the secondary anti-rabbit antibody linked to horseradish peroxidase and developed using the enhanced chemiluminescence (ECL) method according to the manufacturer's protocol. The molecular masses of the receptor bands were determined on the basis of the relative migration of each band to the front of the gel.

Photoaffinity Labeling of the Receptors. As previously described (*27*), membranes from cells expressing the receptors were diluted to a final receptor concentration of about 2 nM in buffer B [50 mM Tris-HCl, 150 mM NaCl, 5 mM EDTA, and 0.2% BSA (w/v), pH 7.4 at 4 °C] and incubated with 4 nM [^{125}I]iodoarylazidoprazosin in the dark for 90 min at 25 °C in the absence or the presence of 10^{-6} M prazosin. After the binding, the membranes were washed twice with buffer B in the dark and finally resuspended in buffer B without BSA. Membranes were exposed to UV light (6 W, 312 nm) for 6 min, washed once using buffer B without BSA, and resuspended in SDS−PAGE sample buffer or in the buffer for endoglycosidase treatment.

In Vitro Translation of the Receptor. The cDNA of the hamster α_{1B}-AR or its mutants was cloned downstream of the β-globin 5′UTR under the regulation of the T7 promoter of the T7-pLink cloning vector. Receptor translation was achieved using the TNT quick-coupled T7 system according to the manufacturer's instructions. The rabbit reticulocyte lysate was incubated with 5 μCi of [^{35}S]methionine and 0.01 μg of DNA in the presence and absence of 0.5 μL of canine microsomal membranes in a total volume of 10 μL for 2.5 h at 37 °C. For SDS−PAGE analysis 3 μL were loaded in each lane.

RESULTS

Electrophoretic Comparison of the α_{1B}-AR in Different Expression Systems. We have previously reported that the α_{1B}-AR can be expressed at high levels of approximately 25 pmol/mg of protein using the SFV system (*25*). The ligand binding and signaling properties of the α_{1B}-AR in SFV-infected BHK-21 cells were similar to those previously reported for the receptor expressed in other cells. To investigate the biochemical properties of the α_{1B}-AR using different recombinant systems, the receptor was transiently expressed in BHK-21 cells and Rat-1 fibroblasts using the SFV vector system or effectene transfections. We also investigated the properties of the α_{1B}-AR permanently expressed in Rat-1 fibroblasts. Western blotting of membrane proteins from control transfected BHK-21 cells or Rat-1 fibroblasts using a polyclonal antibody raised against the C-terminus of the α_{1B}-AR did not identify any cross-reacting nonspecific bands or endogenous receptor bands (Figure 2B, lane 1).

Two main bands could be detected in membranes from effectene-transfected BHK-21 cells and Rat-1 fibroblasts expressing the α_{1B}-AR without a His tag. The larger one migrated around 85 kDa and the smaller band around 67

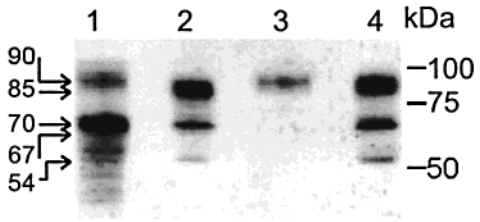

FIGURE 1: Expression of the α_{1B}-AR in different mammalian systems. Western blot analysis of the α_{1B}-AR transiently expressed in BHK-21 cells using the SFV system (lane 1) or effectene transfection (lane 2) and in Rat-1 fibroblasts either stable expressing the α_{1B}-AR (lane 3) or after transient transfection using effectene (lane 4). Receptor expression was 16, 3, 1.5, and 3 pmol/mg of protein, respectively. In each lane 200 fmol of receptors was loaded. Positions of prestained molecular mass markers are indicated on the right, whereas the arrows on the left indicate the mass of the most prominent bands in lanes 1 and 2. The results are representative of several experiments.

kDa in both cell lines (Figure 1, lanes 2 and 4). A weaker band at 54 kDa was also observed. In contrast, in Rat-1 fibroblasts permanently expressing the α_{1B}-AR only one single major receptor band was detected migrating around 90 kDa (Figure 1, lane 3). In membranes derived from BHK-21 cells infected with SFV encoding the His-tagged α_{1B}-AR, Western blotting analysis revealed a number of receptor-specific bands migrating between 42 and 100 kDa, of which two were prominent (Figure 1, lane 1). Of these two bands the larger one migrated around 90 kDa and the smaller around 70 kDa (Figure 1, lane 1). The migration of the bands was slightly slower in this case, probably due to the His tag. In addition, in SFV-infected cells the intensity of the 70 kDa band was stronger than the 90 kDa band, whereas in the cells transfected with effectene the 67 and the 85 kDa bands had nearly equal intensity. However, despite these differences, the migration pattern of the transiently expressed α_{1B}-AR was similar in BHK-21 cells and in Rat-1 fibroblasts transiently expressing the α_{1B}-AR. A similar pattern of bands was also found for the α_{1B}-AR transiently expressed in COS-7 and HEK-293 cells using DEAE-Dextran and calcium phosphate transfections, respectively (results not shown). These findings indicate that the transient overexpression of the α_{1B}-AR results in heterogeneity of the receptor that is not dependent on the expression system used but may arise from co- and posttranslational processing.

Glycosylation of the α_{1B}-AR. The sequence of the α_{1B}-AR contains four potential N-linked glycosylation sites in its N-terminal region (Figure 2A). In addition, a previous study demonstrated that the α_{1B}-AR is endogenously N-glycosylated in smooth muscle cells (*28*). Therefore, the diverse and broad bands observed for the α_{1B}-AR could be due to the various steps and/or to different extents of N-linked glycosylation. Thus, we investigated whether N-linked glycosylation would cause electrophoretic heterogeneity of the receptor protein by treating membranes from cells expressing the α_{1B}-AR with endoglycosidases prior to Western blot analysis. Furthermore, we inhibited the N-linked glycosylation machinery by tunicamycin treatment.

Endo H is an enzyme that selectively removes unprocessed high-mannose oligosaccharides whereas PNGase F also cleaves complex-type N-linked oligosaccharides from glycoproteins. The bands at 85 and 67 kDa were sensitive to the treatment with PNGase F, resulting in the appearance of a band migrating at approximately 58 kDa (Figure 2C, lane 3). In contrast, treatment with Endo H influenced the migration of the 67 kDa band only (Figure 2C, lane 4), indicating that the 67 kDa form is the core glycosylated and the 85 kDa band is fully glycosylated species of the α_{1B}-AR. The faint band at 54 kDa observed in the untreated α_{1B}-AR (Figure 2C, lane 2) or following its treatment with Endo H (Figure 2C, lane 4) is not N-glycosylated.

To inhibit N-linked glycosylation during the biosynthesis of the receptor, transfected BHK-21 cells were grown in the presence of tunicamycin (Figure 2D). The expression level of the α_{1B}-AR measured by ligand binding in membrane preparations from cells treated with tunicamycin was decreased by 50% compared to untreated cells (data not shown). The α_{1B}-AR produced in the presence of tunicamycin migrated as a broad band at approximately 54 kDa, thus confirming that the treatment was efficiently inhibiting N-linked glycosylation (Figure 2D, lane 3). The receptor expressed in the presence of tunicamycin appeared smaller compared to the receptor treated with PNGase F, which migrated around 58 kDa (compare lanes 2 and 3 in Figure 2D). However, in both cases the non-N-glycosylated α_{1B}-AR was not detected as a sharp and homogeneous band by Western blotting.

To further characterize the receptor expressed in transient mammalian expression systems, the biosynthesis of the α_{1B}-AR was studied by pulse−chase labeling of the receptor with [^{35}S]methionine in intact cells. Immunoprecipitation of the [^{35}S]methionine-labeled α_{1B}-AR from transiently transfected BHK-21 cells, Rat-1 fibroblasts, HEK-293 cells, or COS-7 cells resulted in high background and did not allow to distinguish the labeled receptor from endogenous proteins (results not shown). On the contrary, the identification of specifically labeled bands was possible in SFV-infected BHK-21 cells infected with the SFV, because the viral infection reduced the normal host cell protein synthesis due to the efficient replication of the viral RNA, thus allowing a more specific labeling of the α_{1B}-AR.

BHK-21 cells infected with the SFV encoding the His-tagged α_{1B}-AR were labeled with [^{35}S]methionine for 20 min and chased for periods up to 26 h. As shown in Figure 3A, the main labeled species after 0.25 and 1 h of chase had an apparent molecular mass around 70 kDa. Several other weaker bands migrating with apparent lower molecular mass (50 and 54 kDa) were also observed. At longer times of chase, the intensity of these bands decreased whereas in parallel a 90 kDa band appeared peaking at around 4 h (Figure 3D). Similar results were obtained after immunoprecipitation of the receptor with an antibody raised against its N-terminus (results not shown). To further investigate the nature of the 70 and 90 kDa bands, the cells were labeled with [^{3}H]glucosamine. As shown in Figure 4 (lane 1), both bands of the wild-type receptor were labeled by [^{3}H]-glucosamine. The endoglycosidase treatment identified the 70 kDa band as the core glycosylated form and the 90 kDa form as the complex N-glycosylated receptor (Figure 4, lanes 2 and 3). The main receptor species identified in metabolic labeling experiments are similar to those revealed by Western blotting in both BHK-21 and Rat-1 fibroblasts (Figure 1). The 54 kDa band detected by Western blotting (Figure 1) was not labeled by [^{3}H]glucosamine, thus confirming that it represents the nonglycosylated receptor form.

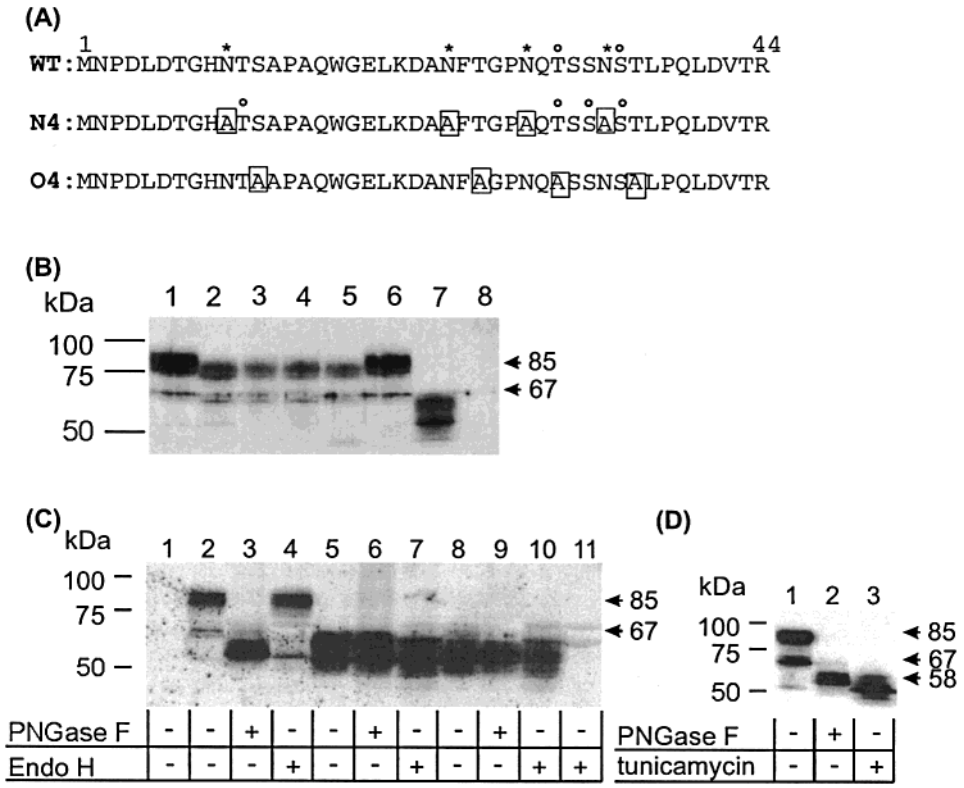

FIGURE 2: Expression of the α_{1B}-AR and its glycosylation-deficient mutants. (A) Amino acid sequence of the N-terminus of the α_{1B}-AR and of the N4 and O4 mutants in which the alanine substitutes are indicated by boxes. Asterisks indicate the potential N-linked glycosylation sites that are mutated to alanines in the N4 mutant; small circles indicate the theoretical O-linked glycosylation sites in the wild-type receptor and in the N4 mutant. (B) Western blot analysis of the α_{1B}-AR (lanes 1 and 6) and the N10A (lane 2), the N24A (lane 3), the N29A (lane 4), the N34A (lane 5), and the N4 (lane 7) mutants. Lane 8 contains membranes from cells transfected with empty vector. (C) Western blot analysis of the α_{1B}-AR (lanes 3 and 4) and the N4 (lanes 5−7) and O4 mutants (lanes 8−10). The membranes were treated with endoglycosydases as indicated. Lane 1 contains membranes from cells transfected with empty vector; lane 11 contains Endo H, showing two faint nonspecific bands. (D) Western blot analysis of the α_{1B}-AR expressed in the absence (lanes 1 and 2) or presence (lane 3) of tunicamycin at 5 μg/mL. In both (B) and (C), BHK-21 cells were transiently transfected with effectene. In each lane 200 fmol of receptors was loaded. Positions of prestained molecular mass markers are indicated on the left. The results are representative of several experiments.

Characterization of Glycosylation-Deficient Mutants of the α_{1B}-AR. To further characterize N-linked glycosylation, we constructed α_{1B}-AR mutants lacking potential N-linked glycosylation sites. The asparagines of the four N-linked glycosylation consensus sites (N-X-S/T) (Figure 2A) were mutated into alanine, individually and in different combinations. Each individual mutation had a small effect on the migration of the receptor based on SDS−PAGE, which was more pronounced when the different mutations were combined (Figure 2B, compare lanes 2−5 with lane 7). This suggests that all four asparagines are used as N-linked glycosylation sites of the α_{1B}-AR. Therefore, only the receptor mutant carrying the mutation of all four asparagines named N4 was used for further studies.

The His-tagged receptor N4 mutant was expressed in BHK-21 cells using the SFV system to investigate the biosynthesis in cells labeled with [^{35}S]methionine. Surprisingly, the N4 mutant expressed two main bands with apparent molecular mass around 56 and 64 kDa at later times of chase (Figure 3B), suggesting that other co- and posttranslational modification may influence its migration. We therefore investigated whether the α_{1B}-AR could become modified by O-linked carbohydrates.

The sequence of α_{1B}-AR was analyzed by the O-linked glycosylation database O-GlycBase (v5.00) (*29*) to determine whether it could become O-linked glycosylated despite the fact that there is no clearly defined consensus site for O-linked glycosylation. This database contains the entry of 198 O-linked glycosylated proteins and uses this information by a computational algorithm for the prediction of new sites. It is known that the presence of several Ser/Thr and Pro favors O-linked glycosylation. Two potential O-glycosylation sites were predicted in the N-terminus of the wild-type α_{1B}-AR, and two additional sites were predicted in the N4 mutant (Figure 2A) as a result of the mutations. We therefore constructed a receptor mutant named O4 carrying the mutations of Ser/Thr of all four N-X-S/T motifs as shown in Figure 2A. The O4 mutant contained no putative N- or O-linked glycosylation site. Similar to the N4 mutant, the His-tagged O4 mutant expressed in cells labeled with [^{35}S]-methionine also exhibited two bands migrating around 50 and 58 kDa at later times of chase (Figure 3C).

Western blotting of membranes from BHK-21 cells expressing the N4 and O4 mutants revealed that both receptors migrated as broad bands between 49−70 and 49−65 kDa, respectively (Figure 2B, lanes 5 and 8). Both mutants were insensitive to Endo H and PNGase F, indicating that N-glycosylation was abolished by the mutations (Figure 2C, lanes 6 and 7 and lanes 9 and 10).

In contrast to the wild-type receptor, the N4 and O4 mutants were not labeled by [^{3}H]glucosamine (Figure 4, lanes 4 and 5). Since *N*-acetylglucosamine is not always found in O-linked carbohydrates, the wild-type receptor and its mutants were immunoprecipitated from cells labeled with

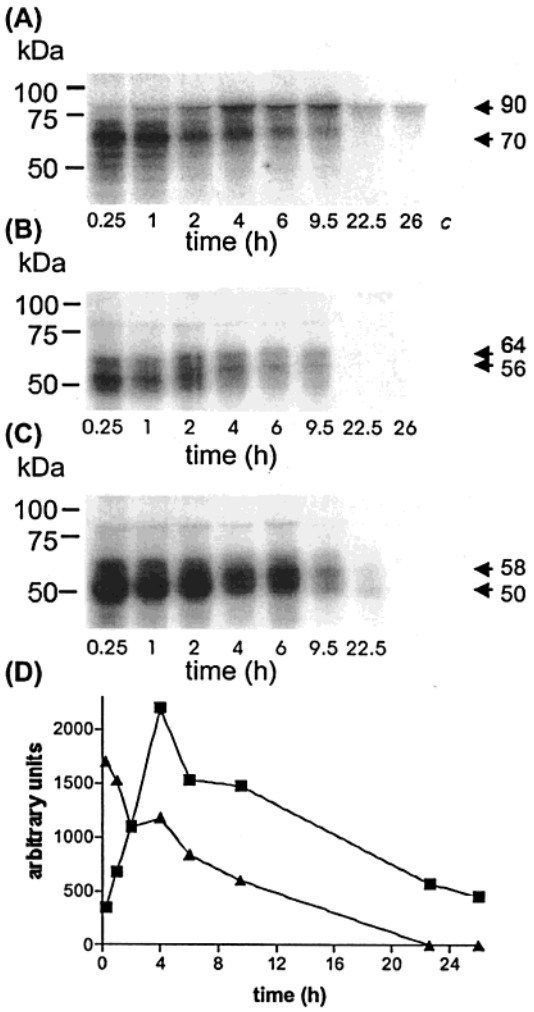

FIGURE 3: Pulse−chase analysis of the α_{1B}-AR and its N-linked glycosylation-deficient mutants. BHK-21 cells infected with the SFV encoding for the His-tagged α_{1B}-AR (A) and N4 (B) or O4 (C) mutants were labeled for 20 min with 100 μCi/mL [^{35}S]-methionine and chased for different times. Cells were solubilized as described in Experimental Procedures, and 500000 dpm of each sample was immunoprecipitated prior to the SDS−PAGE. The dried gels were exposed for 2 days to X-ray films for autioradiography. Positions of prestained molecular mass markers are indicated on the left, whereas the arrows on the right indicate the mass of the two most prominent bands at 9.5 h of chase. In (D), the gel in (A) was analyzed using the Molecular Imager FX and the Quantity One 4.0.3 software (Bio-Rad) for quantifying the radioactivity of different receptor bands that is expressed as arbitrary units and shows the radioactivity incorporated in the 90 kDa (■) and 70 kDa (▲) bands of the α_{1B}-AR-His at each time of chase. The results are representative for two to three experiments.

[^{3}H]galactose. Whereas the wild-type receptor was specifically labeled with [^{3}H]galactose, no incorporation was observed for the N4 and O4 mutants (results not shown). The fact that no labeling with either [^{3}H]glucosamine or [^{3}H]-galactose was observed in the N4 mutant as well as in the wild-type receptor digested by PNGase F (Figure 4, lanes 4 and 2) suggests that the α_{1B}-AR is not modified by O-linked oligosaccharides. This is also supported by the fact that sequential treatment with neuraminidase and *O*-glycosidase after PNGase F did not change the migration pattern either of the wild-type α_{1B}-AR or of the N4 and O4 mutants analyzed by SDS−PAGE and Western blotting (results not shown).

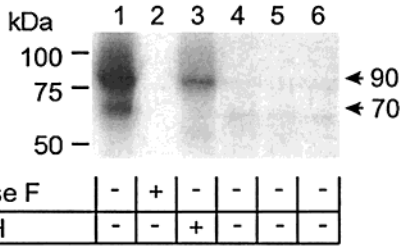

FIGURE 4: [^{3}H]Glucosamine labeling of the α_{1B}-AR and its glycosylation-deficient mutants. BHK-21 cells infected with SFV encoding for the His-tagged α_{1B}-AR (lanes 1−3) and the N4 (lane 4) or O4 (lane 5) mutants were labeled for 5.5 h with [^{3}H]-glucosamine. Membranes expressing the His-tagged α_{1B}-AR were treated with endoglycosidases as indicated (lanes 2 and 3). Lane 6 contains membranes from noninfected cells. Cells were solubilized as described in Experimental Procedures, and 500000 dpm of each sample was immunoprecipitated prior to SDS−PAGE. The dried gel was exposed for 15 days to a X-ray film for autoradiography. Receptor expression was 3 and 1.5 pmol/mg of protein for cells grown in the absence or presence of tunicamycin, respectively. In each lane 200 fmol of receptors was loaded. Positions of prestained molecular mass markers are indicated on the left. The results are representative of two experiments.

Palmitoylation and Phosphorylation of the α_{1B}-AR. In addition to glycosylation, other important posttranslational modifications of different GPCRs are palmitoylation and phosphorylation. There is recent evidence that the α_{1B}-AR is palmitoylated at two cysteines in the C-terminus (*30*). To assess the potential role of palmitoylation on the migration pattern of the receptor, the two cysteines were mutated into alanine in the wild-type α_{1B}-AR as well as in the N4 mutant. Western blotting analysis indicated that mutating the palmitoylation sites had no significant effect on receptor migration (results not shown).

We have previously reported that a stretch of eight serines in the C-tail of the α_{1B}-AR is the substrate for phosphorylation mediated by protein kinase C and G protein-coupled receptor kinases (*31*). This was demonstrated by the fact that the M8 mutant carrying mutations of these serines was profoundly impaired in its ability to undergo phosphorylation and desensitization. To investigate the effect of receptor phosphorylation on the migration of the α_{1B}-AR on SDS−PAGE, we compared the Western blotting of the wild-type receptor and of the M8 mutant treated with PNGase F (Figure 5A). Like the wild-type α_{1B}-AR, the M8 mutant displayed the fully glycosylated and the core glycosylated forms which were decreased in size by PNGase F (Figure 5A, lanes 6 and 8). However, the receptor species of the M8 mutant displayed a slightly higher mobility compared to the wild-type receptor bands probably due to the lack of phosphorylation resulting from the mutation. The enzymatic dephosphorylation of the wild-type α_{1B}-AR treated or not with PNGase F by calf intestinal alkaline phosphatase (AP) resulted also in a small downward shift of its size (Figure 5A, compare lanes 2 and 3 and lanes 4 and 5). As expected, AP had no effect on the M8 mutant (Figure 5A, compare lanes 6 and 7 and lanes 8 and 9). This demonstrates that receptor phosphorylation contributes to the structural heterogeneity of the α_{1B}-AR expressed in transient systems, as it can be observed in SDS−PAGE.

This conclusion is further supported by the results on the double mutants N4/M8 and O4/M8 in which the mutations of the phosphorylation sites were introduced in the N-linked

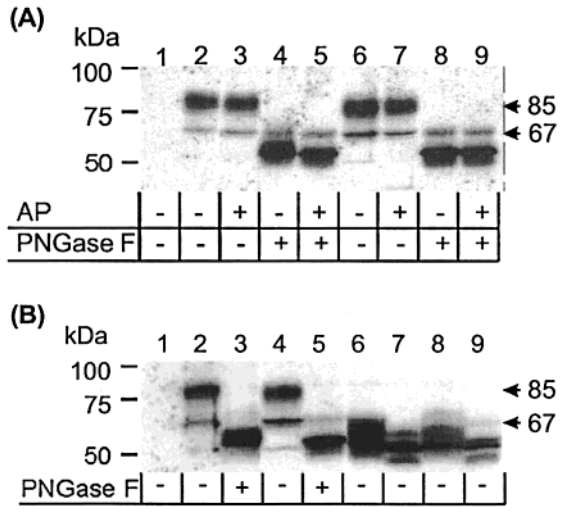

FIGURE 5: Expression of the α_{1B}-AR and its phosphorylation- and/or glycosylation-deficient mutants. Western blot analysis of the α_{1B}-AR and of different mutants transiently expressed in BHK-21 cells using effectene. (A) shows the analysis of the α_{1B}-AR (lanes 2−5) and of the M8 mutant (lanes 6−9). The membranes were treated with PNGase F and/or alkaline phosphatase (AP) as indicated. SDS−PAGE was performed using a 7−12% gradient gel. Lane 1 contains membranes from cells transfected with empty vector. In each lane 100 fmol of receptors was loaded. The 64 kDa band insensitive to PNGase F in lanes 4, 5, 8, and 9 was occasionally observed in different experiments. This band might be nonspecific or result from incomplete digestion by PNGase F. (B) shows the analysis of the α_{1B}-AR (lanes 2 and 3) and the M8 (lanes 4 and 5), N4 (lane 6), N4/M8 (lane 7), O4 (lane 8), and O4/M8 (lane 9) mutants. Lane 1 contains membranes from cells transfected with empty vector. The membranes were treated with PNGase F as indicated. SDS−PAGE was performed using a 8−13% gradient gel. In each lane 200 fmol of receptors was loaded. Positions of prestained molecular mass markers are indicated on the left. The results are representative of three experiments.

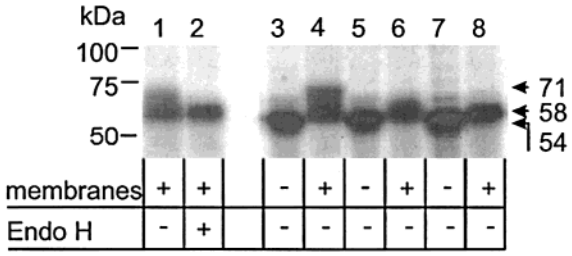

FIGURE 6: In vitro translation of the α_{1B}-AR and its mutants lacking the phosphorylation or glycosylation sites. The α_{1B}-AR (lanes 1−4) and the O4 (lanes 5 and 6) and the O4/M8 (lanes 7 and 8) mutants were in vitro translated in the absence or presence of microsomal membranes as indicated. The in vitro translated α_{1B}-AR in the presence of membranes was also treated with Endo H. The dried gel was exposed for 7 h to X-ray films for autoradiography.

glycosylation-deficient mutants. Though on Western blots the N4/M8 and O4/M8 mutants still displayed several bands, these were sharper than the bands of the N4 and O4 receptors (Figure 5B, compare lanes 6 and 7 and lanes 8 and 9).

In Vitro Translation of the α_{1B}-AR and Its Mutants. To further investigate the heterogeneity of the receptor on SDS−PAGE, the wild-type α_{1B}-AR and the O4 and the O4/M8 mutants were also analyzed by in vitro translation (Figure 6). The translation of the three receptors without microsomal membranes resulted in a single band migrating around 54 kDa (Figure 6, lanes 3, 5, and 7). The addition of canine microsomal membranes shifted the translated protein toward higher molecular mass for all three receptors, but to different extents. The wild-type α_{1B}-AR translated in the presence of microsomal membranes migrated as a broad band between 58 and 71 kDa (Figure 6, lanes 1 and 4) and was sensitive to Endo H that shifted its molecular mass to 58 kDa (Figure 6, lane 2). This suggests that the wild-type receptor translated in the presence of microsomal membranes was a mixture of core glycosylated and nonglycosylated receptor, as expected in this system (*32*). Despite not being N-glycosylated, the O4 mutant in the presence of microsomal membranes migrated as a band of approximately 58 kDa, which is larger than that in the absence of membranes (54 kDa), suggesting that other cotranslational modifications may occur in vitro (Figure 6, compare lanes 5 and 6). Interestingly, the band corresponding to the O4/M8 mutant in the presence of membranes was slightly smaller than that of the O4 mutant (Figure 6, compare lanes 8 and 6). The slightly higher mobility of the O4/M8 might result from the fact that it is missing most of the phosphorylation sites, thus suggesting that phosphorylation may occur also at the in vitro translated receptor. In fact, the reticulocyte lysate has been shown previously to contain some phosphorylation activity and could be the source of rather nonspecific phosphorylation in this system (*33*). Despite the fact that the O4/M8 mutant lacked the N-linked glycosylation and most phosphorylation sites, the receptor translated in the presence of membranes migrated slower than that translated in the absence (Figure 6, compare lanes 7 and 8).

Functional Characterization of Co- and Posttranslational Modification of the α_{1B}-AR. To assess the effect of the different co- and posttranslatinal modification on receptor function, the receptor mutants were expressed in BHK-21 cells and tested for their ligand binding and signaling properties. As shown in Table 1, mutations of the glycosylation and/or phosphorylation sites did not significantly change the expression and ligand affinity as well as the inositol phosphate response of the receptor.

To further investigate the expression of the N4 and O4 mutants at the cell surface, we constructed receptor−GFP fusion proteins and transiently expressed them in BHK-21 and HEK-293 cells using effectene. The ligand binding and signaling properties of the receptors fused to GFP were similar to those of the wild-type α_{1B}-AR (Table 1). As shown in Figure 7, in cells expressing the α_{1B}-AR fused to GFP the fluorescence was distributed in the cytoplasm as well as at the plasma membrane, thus suggesting that a significant fraction of the wild-type receptor is intracellular. A similar distribution of the fluorescence was observed in cells expressing the N4 or O4 mutants fused to GFP (Figure 7).

To investigate the ability of the different receptor bands to bind ligands, we performed photoaffinity labeling of membranes expressing the α_{1B}-AR or its mutants with [^{125}I]-iodoarylazidoprazosin and analyzed them by SDS−PAGE. Photoaffinity labeling of membranes from BHK-21 cells expressing the His-tagged or wild-type α_{1B}-AR revealed two main labeled bands (Figure 8, lanes 1 and 4) corresponding to the fully and core glycosylated receptor form (compare with Figure 1). The labeling of these bands was specific since it could be displaced by 10^{-6} M prazosin (Figure 8, lanes 2 and 5). The relative intensity of the core glycosylated to the fully glycosylated band of the His-tagged α_{1B}-AR was weaker after photoaffinity labeling as compared to Western blotting (compare Figure 8, lane 1, with Figure 1, lane 1).

Table 1: Functional Properties of the α_{1B}-AR and Its Mutants[a]

receptor	B_{max} (pmol/mg of protein)	[^{125}I]HEAT K_D (pM)	adrenaline K_I (μM)	prazosin K_I (nM)	IP (% above basal)	adrenaline EC_{50} (nM)
α_{1B}-AR	4.9 ± 0.9	77 ± 3	4.7 ± 1.2	0.65 ± 0.1	87 ± 7	39 ± 14
N4	7.9 ± 2	66 ± 9	3.9 ± 0.1	1 ± 0.1	77 ± 6	8.3 ± 4
O4	4.6 ± 0.8	76 ± 1	4.2 ± 0.7	0.5 ± 0.1	94 ± 13	23 ± 10
M8	4.7 ± 1	104 ± 10	4.8 ± 0.1	0.64 ± 0.1	86 ± 6	26 ± 6
N4/M8	5.8 ± 1	118 ± 13	4.7 ± 0.7	0.61 ± 0.1	89 ± 15	15 ± 3
O4/M8	4.5 ± 1.5	117 ± 13	5.0 ± 0.8	0.65 ± 0.1	101 ± 16	16 ± 0.2
N4-GFP	5.3 ± 1	75 ± 6	2.3 ± 0.3	0.61 ± 0.1	69 ± 7	51 ± 8
O4-GFP	4.6 ± 1	62 ± 7	2.2 ± 0.1	0.61 ± 0.1	78 ± 10	45 ± 5

[a] The wild-type α_{1B}-AR and its mutants were expressed in BHK-21 cells using effectene transfection. Saturation binding of [^{125}I]HEAT was performed on membrane preparations. Inositol phosphate (IP) accumulation was measured following incubation with 100 μM adrenaline for 45 min and is expressed as the percent increase above the basal levels which were similar for the cells expressing the different receptors. K_I values were assessed in competition binding experiments using 80 pM [^{125}I]HEAT. The EC_{50} values of adrenaline were assessed using different concentrations from 10^{-10} to 10^{-4} M. Values represent means ± SE from three experiments for the receptor mutants and from three to seven experiments for the α_{1B}-AR.

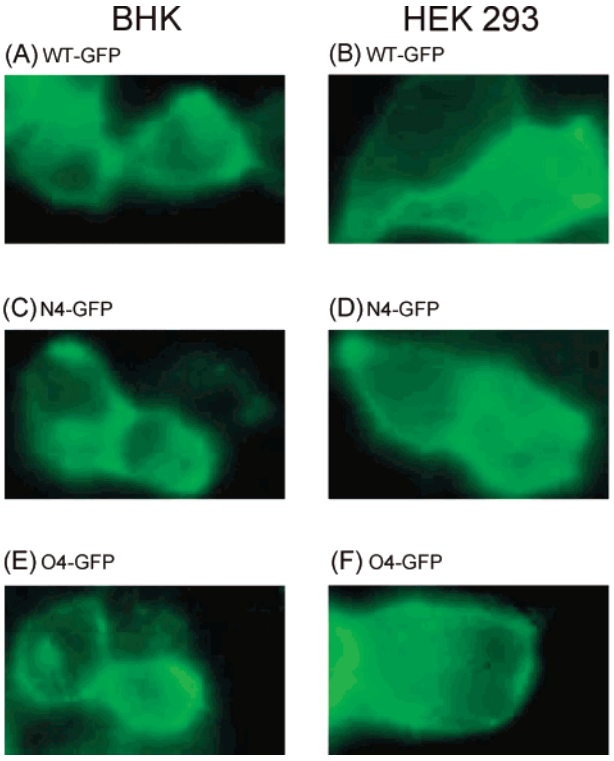

FIGURE 7: Receptor−GFP fusion proteins expressed in BHK-21 and HEK-293 cells. The GFP was fused at the C-terminus of the α_{1B}-AR (WT) and of its mutants N4 and O4. Cells transiently transfected using effectene were analyzed by fluorescence microscopy. The results are representative of several experiments.

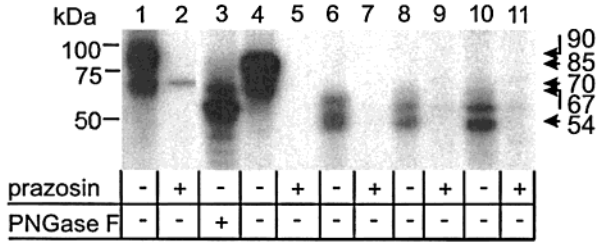

FIGURE 8: Photoaffinity labeling of the α_{1B}-AR and its mutants lacking the phosphorylation or glycosylation sites or both. The His-tagged α_{1B}-AR was expressed in BHK-21 cells using the SFV system (lanes 1 and 2) or effectene (lanes 3−5). The N4 (lanes 6 and 7), O4 (lanes 8 and 9), and O4/M8 (lanes 10 and 11) mutants were transiently expressed in BHK-21 cells using effectene. Membranes were incubated with [^{125}I]iodoarylazidoprazosin in the absence or presence of prazosin (10^{-6} M). Membranes expressing the His-tagged α_{1B}-AR were also digested with PNGase F (lane 3). The dried gel was exposed for 6 h to a X-ray film for autoradiography. Positions of prestained molecular mass markers are indicated on the left. The results are representative of two experiments.

This suggests that part of the core glycosylated α_{1B}-AR form migrating at 70 kDa does not bind ligands.

The N4, the O4, and the O4/M8 mutants were also specifically labeled by [^{125}I]iodoarylazidoprazosin. For all three receptor mutants, the labeled receptor displayed two main bands, similar to those detected by Western blotting (compare Figure 8, lanes 6, 8, and 10, with Figure 5B, lanes 6, 8, and 9). This indicates that the multiple bands observed on the Western blot represent, at least in part, the functional receptor.

To identify which receptor bands were expressed at the cell surface, the α_{1B}-AR and its glycosylation-deficient mutants were expressed in BHK-21 cells labeled with [^{35}S]-methionine and immunoprecipitated from whole cells with antibodies raised against the N-terminus of the receptor. The bands immunoprecipitated for both the wild-type and mutated receptors were similar to the two prominent bands identified by the photoaffinity labeling (results not shown). This might indicate that both the complex and core glycosylated receptor species are expressed at the cell surface. However, this would be somehow intriguing since it has been shown that very little core glycosylated GPCR reaches the cell surface. In fact, we cannot rule out that cells infected with the SFV are not fully intact, thus allowing the antibodies to penetrated into the cytosol and bind to the intracellular pool of the receptor. Another hypothesis to explain these findings is that the core glycosylated form of the receptor is mainly intracellular, but it can still bind the photoaffinity ligand.

DISCUSSION

The principal implications of this study are twofold. First, it identifies the basic steps involved in the maturation of the α_{1B}-AR. Second, it characterizes the co- and posttranslational modifications involved in the structural heterogeneity of the receptor expressed in different mammalian systems as it is observed in SDS−PAGE.

The α_{1B}-AR expressed in vitro and in vivo undergoes N-linked glycosylation as demonstrated by its sensitivity to endoglycosidases as well as by the effect of tunicamycin on receptor maturation in intact cells (Figure 2). The kinetic

results from pulse−chase labeling experiments demonstrate that the His-tagged α_{1B}-AR is initially synthesized as a 70 kDa core glycosylated precursor that is converted to the 90 kDa mature form of the receptor with a half-time of about 2 h (Figure 3). Other weaker bands with apparent lower molecular mass identified after the shortest time of chase might include the nonglycosylated receptor whose molecular mass, as calculated from its amino acid sequence, is 56 kDa.

N-Linked glycosylation of the α_{1B}-AR occurs at four asparagines on the N-terminus of the receptor as demonstrated by the fact that the N4 and O4 mutants lacking the consensus sites for N-linked glycosylation were totally insensitive to endoglycosidases (Figure 2). An important finding of our study is that mutations of the N-linked glycosylation sites did not significantly change the ligand binding and signaling properties of the α_{1B}-AR (Table 1) or its ability to be expressed at the cell surface (Figure 7). In contrast, the treatment of cells expressing the α_{1B}-AR with tunicamycin decreased receptor expression by about 50%. This could be due to the fact that, in addition to inhibiting N-linked glycosylation, tunicamycin can inhibit protein synthesis or stimulate protein degradation as it was recently shown for apolipoprotein B (*34*).

Our results indicate that different extents of N-linked glycosylation are among the phenomena causing the electrophoretic heterogeneity of the α_{1B}-AR when transiently overexpressed in mammalian cells. In fact, the α_{1B}-AR transiently expressed in BHK-21 and Rat-1 fibroblast displayed three main bands that were identified as non-N-linked and core and complex N-linked glycosylated forms (Figure 1, lanes 2 and 4). In contrast, if the receptor was expressed in stable transfected Rat-1 fibroblast, only the complex N-glycosylated form was detected by Western blotting (Figure 1, lane 3). These results indicate that in the transient expression systems the maturation of the α_{1B}-AR is incomplete, probably because the overexpressed receptor protein saturates the protein processing machinery of the host cell. Interestingly, the receptor expressed in BHK-21 cells using the SFV system showed a pattern very similar to that expressed in various cells (BHK-21, Rat-1, COS-7, and HEK-293) using conventional transient transfection systems (results not shown), but additional fainter bands of molecular mass smaller than 54 kDa appeared (Figure 1, lane 1). These bands were also detected in the pulse−chase labeling experiments (Figure 3). It is possible that these receptor forms with molecular mass smaller than that expected for the nonglycosylated receptor are the result of receptor degradation. In fact, recently it has been shown that a large part of the de novo synthesized δ opioid receptor expressed in stable transfected HEK-293 cells becomes ubiquitinated and degraded in the proteasome (*35*).

An intriguing finding of our study is that α_{1B}-AR lacking the N-linked oligosaccharides following the digestion with endoglycosidases or treatment with tunicamycin or mutagenesis of the N-linked glycosylation consensus sites were never detected as simple but as multiple bands on SDS−PAGE (Figure 2B,C). In particular, the N4 and O4 mutants displayed multiple bands on Western blots and a doublet both in pulse−chase and in photoaffinity labeling experiments (Figures 2, 3, and 8).

This differs from the results obtained with other GPCRs such as the H2 histamine receptor and the AT_{1a} receptor for angiotensin in which mutating the N-linked glycosylation sites resulted in a single fairly homogeneous receptor product detected by Western blotting (*9, 10*). However, the N-linked glycosylation-deficient mutant of the V2 vasopressin migrated as two bands, one of which was found to be modified by O-linked glycans (*15*). Our findings do not support the hypothesis that the α_{1B}-AR undergoes O-linked glycosylation and that this modification contributes to the heterogeneity of the receptor. This was based on four main lines of evidence. First, no incorporation of either [^{3}H]glucosamine or [^{3}H]galactose could be observed either in the N4 and O4 receptor mutants or in the wild-type receptor after its treatment with PNGase F (Figure 4). Second, the migration pattern of the O4 mutant lacking both N- and O-linked glycosylation sites was similar to that of the N4 mutant. Third, treatments with neuraminidase and *O*-glycosidase after PNGase F did not change the migration pattern of the wild-type α_{1B}-AR (results not shown). Fourth, the mutation of two serines (Ser 421 and Ser 423) that could be a site for O-glycosylation in the C-tail of the receptor did not change the migration pattern of the deglycosylated α_{1B}-AR or of its mutants N4, O4, and O4/M8 (results not shown).

However, despite the fact that the migration pattern of the N4 and O4 receptors was overall similar, it was not identical. As seen in Figure 3, the sizes of the bands corresponding to the O4 mutant were consistently smaller than those of the N4. This difference in mobility could support the presence of O-glycosylation that cannot be entirely ruled out by the negative results of our experiments. Another explanation of this difference may be that the mutations of four asparagines in the N4 mutant and of four serines/threonines in the O4 mutant have different impact on the migration of the receptor protein on SDS−PAGE.

We also excluded that receptor palmitoylation influenced the heterogeneity on SDS−PAGE of the α_{1B}-AR. This was demonstrated by the finding that mutating the two palmitoylation sites at the C-terminus of the receptor did not modify the migration pattern of the wild-type α_{1B}-AR or of the N4 mutant (results not shown). In contrast, receptor phosphorylation was found to influence the migration of the α_{1B}-AR. In fact, the α_{1B}-AR treated with alkaline phosphatase and the M8 receptor mutant lacking eight phosphorylation sites in its C-tail displayed a slightly higher mobility in SDS−PAGE compared to the untreated receptor (Figure 5A). In addition, the N4/M8 and O4/M8 mutants lacking both the N-linked glycosylation and phosphorylation sites appeared as defined bands much sharper than the nonglycosylated forms of the receptor (Figure 5B, compare lanes 7 and 9 with lanes 3, 6, and 8). Even though phosphorylation contributes to receptor heterogeneity, other factors should contribute to the fact that the O4/M8 mutant displayed multiple bands.

We exclude that the two main bands corresponding to the N4 and O4 in pulse−chase labeling experiments (Figure 3) result from proteolysis of the receptor, since both bands could also be immunoprecipitated by antibodies against the N-terminus of the α_{1B}-AR (results not shown). Pulse−chase experiments indicated that, despite the lack of the N-linked glycosylation, the N4 and O4 mutants could also undergo some time-dependent maturation, suggesting that other posttranslational modifications, which remain unknown, occur at the receptor. However, photoaffinity labeling of the

N4, O4 and O4/M8 receptors revealed that the two main bands were functional since they were specifically labeled by [^{125}I]iodoarylazidoprazosin (Figure 8).

Whereas the migration patterns on SDS−PAGE observed for the α_{1B}-AR mutants deficient in N-linked glycosylation expressed in intact cells were quite heterogeneous, the in vitro translated receptors migrated as fairly homogeneous bands (compare Figures 5B and 6). This indicates that the heterogeneity of the receptor mutants cannot be attributed to insufficient denaturation of the protein or other technical artifacts that should have influenced also the migration of the in vitro translated receptors. To achieve denaturation of the protein, the receptor was incubated in sample buffer containing 2% SDS and 5% β-mercaptoethanol for 1 h at room temperature or at 4 °C overnight prior the SDS−PAGE. Longer incubations or the addition of 10% DTT did not have any effect on the migration pattern of the α_{1B}-AR. Heating the samples prior to SDS−PAGE resulted in the formation of large aggregates of the proteins. Therefore, the reasons for this heterogeneity remain elusive. One possibility is that the mutated receptors overexpressed in intact cells undergo incomplete maturation and/or enhanced degradation that result(s) in multiple receptor bands. Another possibility is that the mutations of the glycosylation sites of the α_{1B}-AR, despite not having significant effects on receptor function, modify the structural properties of the protein, thus affecting its migration pattern. It is also possible that the α_{1B}-AR undergoes other co- and posttranslational modifications not yet identified that become more apparent in the receptor mutants lacking the N-linked glycosylation sites.

An important finding of our study is that a large part of the α_{1B}-AR overexpressed using the SFV system is in its mature fully glycosylated form. Several recombinant systems have been used so far to express high levels of GPCRs including yeast, bacteria, and insect cells (*36*, *37*). The impairment in posttranslational modifications of the protein expressed in nonmammalian cells might represent a disadvantage for the proper folding and function of GPCRs. However, overexpression of GPCRs in mammalian cells has often been limited by low efficiency of transfection and expression levels. These limits have been recently, at least in part, overcome by viral vectors such as the SFV that has been successfully used to overexpress soluble as well as membrane proteins in a wide range of host cells (*38*). Recent studies have shown that this system could also be used to obtain high-level expression of some GPCRs (*25*, *39*). Our findings further support this evidence, demonstrating that the SFV system is a useful tool to produce large amounts of functional and fully processed α_{1B}-AR protein suitable for biochemical and structural studies.

The specific steps involved in the processes of receptor maturation and processing have been extensively explored only for a limited number of GPRCs (*5*, *16*, *35*, *40*), and the results of this study contribute to expand our knowledge in this field. A better understanding of these processes should also allow to improve the strategies to express and purify large amounts of GPRCs suitable for structural studies of the receptor proteins.

ACKNOWLEDGMENT

We acknowledge Monique Nenniger-Tosato for excellent technical assistance, Dr. Laura Stanasila for the construction of the cDNA encoding the α_{1B}-adrenergic receptor−GFP fusion protein, Prof. Hitoshi Kurose for the kind supply of anti-α_{1B}-AR antibody, and Prof. Käthi Geering for helpful discussions.

REFERENCES

1. Palczewski, K., Kumasaka, T., Hori, T., Behnke, C. A., Motoshima, H., Fox, B. A., Le Trong, I., Teller, D. C., Okada, T., Stenkamp, R. E., Yamamoto, M., and Miyano, M. (2000) *Science 289*, 739−745.
2. Rands, E., Candelore, M. R., Cheung, A. H., Hill, W. S., Strader, C. D., and Dixon, R. A. (1990) *J. Biol. Chem. 265*, 10759−10764.
3. Garcia Rodriguez, C., Cundell, D. R., Tuomanen, E. I., Kolakowski, L. F., Jr., Gerard, C., and Gerard, N. P. (1995) *J. Biol. Chem. 270*, 25178−25184.
4. Liu, X., Davis, D., and Segaloff, D. L. (1993) *J. Biol. Chem. 268*, 1513−1516.
5. Nagayama, Y., Nishihara, E., Namba, H., Yamashita, S., and Niwa, M. (2000) *J. Pharmacol. Exp. Ther. 295*, 404−409.
6. Ray, K., Clapp, P., Goldsmith, P. K., and Spiegel, A. M. (1998) *J. Biol. Chem. 273*, 34558−34567.
7. Karpa, K. D., Lidow, M. S., Pickering, M. T., Levenson, R., and Bergson, C. (1999) *Mol. Pharmacol. 56*, 1071−1078.
8. Boer, U., Neuschafer-Rube, F., Moller, U., and Puschel, G. P. (2000) *Biochem. J. 350*, 839−847.
9. Deslauriers, B., Ponce, C., Lombard, C., Larguier, R., Bonnafous, J. C., and Marie, J. (1999) *Biochem. J. 339*, 397−405.
10. Fukushima, Y., Oka, Y., Saitoh, T., Katagiri, H., Asano, T., Matsuhashi, N., Takata, K., van Breda, E., Yazaki, Y., and Sugano, K. (1995) *Biochem. J. 310*, 553−558.
11. Bisello, A., Greenberg, Z., Behar, V., Rosenblatt, M., Suva, L. J., and Chorev, M. (1996) *Biochemistry 35*, 15890−15895.
12. Innamorati, G., Sadeghi, H., and Birnbaumer, M. (1996) *Mol. Pharmacol. 50*, 467−473.
13. Kaushal, S., Ridge, K. D., and Khorana, H. G. (1994) *Proc. Natl. Acad. Sci. U.S.A. 91*, 4024−4028.
14. Webel, R., Menon, I., O'Tousa, J. E., and Colley, N. J. (2000) *J. Biol. Chem. 275*, 24752−24759.
15. Sadeghi, H., and Birnbaumer, M. (1999) *Glycobiology 9*, 731−737.
16. Petaja-Repo, U. E., Hogue, M., Laperriere, A., Walker, P., and Bouvier, M. (2000) *J. Biol. Chem. 275*, 13727−13736.
17. Nakagawa, M., Miyamoto, T., Kusakabe, R., Takasaki, S., Takao, T., Shichida, Y., and Tsuda, M. (2001) *FEBS Lett. 496*, 19−24.
18. Ferguson, S. S. (2001) *Pharmacol. Rev. 53*, 1−24.
19. O'Dowd, B. F., Hnatowich, M., Caron, M. G., Lefkowitz, R. J., and Bouvier, M. (1989) *J. Biol. Chem. 264*, 7564−7569.
20. Kennedy, M. E., and Limbird, L. E. (1994) *J. Biol. Chem. 269*, 31915−31922.
21. Gao, Z., Ni, Y., Szabo, G., and Linden, J. (1999) *Biochem. J. 342*, 387−395.
22. Soskic, V., Nyakatura, E., Roos, M., Muller-Esterl, W., and Godovac-Zimmermann, J. (1999) *J. Biol. Chem. 274*, 8539−8545.
23. Moffett, S., Rousseau, G., Lagace, M., and Bouvier, M. (2001) *J. Neurochem. 76*, 269−279.
24. Lundstrom, K., Mills, A., Buell, G., Allet, E., Adami, N., and Liljestrom, P. (1994) *Eur. J. Biochem. 224*, 917−921.
25. Scheer, A., Bjorklof, K., Cotecchia, S., and Lundstrom, K. (1999) *J. Recept. Signal Transduct. Res. 19*, 369−378.
26. Cotecchia, S., Ostrowski, J., Kjelsberg, M. A., Caron, M. G., and Lefkowitz, R. J. (1992) *J. Biol. Chem. 267*, 1633−1639.
27. Lattion, A. L., Diviani, D., and Cotecchia, S. (1994) *J. Biol. Chem. 269*, 22887−22893.
28. Sawutz, D. G., Lanier, S. M., Warren, C. D., and Graham, R. M. (1987) *Mol. Pharmacol. 32*, 565−571.
29. Gupta, R., Birch, H., Rapacki, K., Brunak, S., and Hansen, J. E. (1999) *Nucleic Acids Res. 27*, 370−372.

30. Stevens, P. A., Pediani, J., Carrillo, J. J., and Milligan, G. (2001) *J. Biol. Chem. 276*, 35883−35890.
31. Diviani, D., Lattion, A. L., and Cotecchia, S. (1997) *J. Biol. Chem. 272*, 28712−28719.
32. Krieg, P. A., and Melton, D. A. (1984) *Nucleic Acids Res. 12*, 7057−7070.
33. Walter, P., and Blobel, G. (1983) *Methods Enzymol. 96*, 84−93.
34. Liao, W., and Chan, L. (2001) *Biochem. J. 353*, 493−501.
35. Petaja-Repo, U. E., Hogue, M., Laperriere, A., Bhalla, S., Walker, P., and Bouvier, M. (2001) *J. Biol. Chem. 276*, 4416−4423.
36. Grisshammer, R., and Tate, C. G. (1995) *Q. Rev. Biophys. 28*, 315−422.
37. Grunewald, S., Haase, W., Reilander, H., and Michel, H. (1996) *Biochemistry 35*, 15149−15161.
38. Lundstrom, K. (2000) *Res. Adv. Neurochem. 1*, 1−11.
39. Lundstrom, K., Mills, A., Allet, E., Ceszkowski, K., Agudo, G., Chollet, A., and Liljestrom, P. (1995) *J. Recept. Signal Transduct. Res. 15*, 23−32.
40. Kobilka, B. K. (1990) *J. Biol. Chem. 265*, 7610−7618.

BI015790J